

On Subquadratic Architectures: From Applications to Principles

Anamaria-Roberta Hartl^{*1}, Levente Zólyomi^{*1,2}, David Stap², Pieter-Jan Hoedt¹,
Niklas Schmidinger^{1,2}, Lukas Hauenberger^{1,2}, Sebastian Böck², Günter Klambauer^{1,2},
Sepp Hochreiter^{1,2}

¹ Johannes Kepler University Linz ² NXAI GmbH * Equal contribution.

Corresponding authors: Anamaria-Roberta Hartl (hartl@ml.jku.at), Levente Zólyomi (levente.zolyomi@nx-ai.com)

Abstract

Transformers dominate modern sequence modeling, but their quadratic attention incurs substantial computational cost. Subquadratic architectures offer a scalable alternative. However, it remains unclear which designs yield the most effective sequence models. We compare three leading approaches: xLSTM, Mamba-2, and Gated DeltaNet. We evaluate these models on tasks with complex dependencies: (1) code-model pre-training, (2) distillation of code models from large language models, and (3) pre-training of time-series foundation models. Across these settings, xLSTM delivers the strongest overall performance. To explain xLSTM’s advantage, we present a unified formulation and analyze the underlying architectural mechanisms, focusing on state tracking and memory dynamics. Our results show that xLSTM enables more flexible and stable memory correction via its gating scheme. We corroborate these findings on controlled synthetic length-generalization tasks. Overall, our findings indicate that xLSTM’s gains on complex tasks stem from robust state tracking and accumulation.

1 Introduction

Subquadratic architectures as scalable alternatives to Transformers. Transformers (Vaswani et al., 2017) dominate modern sequence modeling and remain the default backbone for foundation models in language, code, and time series. At the same time, their quadratic attention cost has motivated subquadratic alternatives based on recurrent, state-space, and linear-attention mechanisms. Recent hybrid foundation models such as Samba (Ren et al., 2025), Nemotron Nano (NVIDIA, 2025), Kimi Linear (Team, 2025b), and Olmo Hybrid (Merrill et al., 2026b) replace many attention layers with subquadratic sequence operators. This makes the choice of operator central to the design of modern hybrid language models.

Three leading architectures: xLSTM, Mamba-2 and Gated DeltaNet. Several subquadratic architectures have been suggested for a diverse range of tasks (Fichtl et al., 2025). Out of those, xLSTM (Beck et al., 2024) has demonstrated competitive language modeling (Beck et al., 2025) and was shown to Pareto-dominate transformers (Beck et al., 2026). Moreover, it serves as the backbone of TiRex, one of the best-performing time-series foundation models (Auer et al., 2025). Mamba-2 (Dao and Gu, 2024) appears as a core component in competitive hybrid language models (Team, 2025a; Glorioso et al., 2024; Ren et al., 2025; NVIDIA, 2025). Finally, Gated DeltaNet (Yang et al., 2024b) is used in competitive hybrid language models (Team, 2025b; Merrill et al., 2026b), and has been adopted in recent time-series work (Moroshan et al., 2025). While prior work motivates all three architectures as relevant backbones, no head-to-head comparison exists.

A comparison on complex data domains. So far, subquadratic backbones have mostly been compared on standard language modeling and commonsense reasoning benchmarks, where performance differences are small and architectures are hard to differentiate (Yang et al., 2024a; Mishra, 2024). In contrast, prior work has shown that architectural inductive biases diverge sharply on data with

arXiv:2606.12364v1 [cs.LG] 10 Jun 2026

long-range, structured dependencies (Deletang et al., 2023; Liu et al., 2023). We therefore evaluate the operators on *complex data domains*: naturally-occurring data whose generating process imposes such structured dependencies, instantiated here by *code* and *time series* (see Figure 1). On the one hand, code combines language-like tokens with formal structure, including syntax, variable bindings, and scopes (Siems et al., 2026; Merrill et al., 2026b). On the other hand, time series require models to infer and update complex dynamics from continuous-valued histories across heterogeneous domains (Ansari et al., 2024; Das et al., 2024; Auer et al., 2025). We test the sequence backbones under both from-scratch pre-training and Transformer-to-subquadratic distillation (Schmidhuber, 1991; Hinton et al., 2015; Mercat et al., 2024), and additionally evaluate the models on code generation tasks. Across these three settings, xLSTM-based backbones¹ consistently show favorable results, which raises the central question of the paper: *which architectural design choices explain xLSTM’s advantage on complex sequence tasks?*

A unified framework for xLSTM, Mamba-2, and Gated DeltaNet. We explain xLSTM’s advantage by formulating xLSTM, Mamba-2, and Gated DeltaNet into a unified framework (Section 3). This formulation makes the architectures directly comparable at the level where they differ most: how they write, forget, overwrite, and read from state. Our unified formulation identifies a hypothesis that the architectures should differ most on two primitive capabilities: accumulation and state tracking. Our framework motivates to test this hypothesis on controlled synthetic length-generalization tasks (Section 4). Counting tasks isolate accumulation beyond the training length, while state-tracking tasks isolate ordered finite-state updates over sequences. The results support this prediction, where xLSTM can solve both of these task families well beyond its training length. Together, the practical comparisons, unified formulation, and synthetic tasks support the same conclusion: xLSTM’s gains on tasks with complex dependencies stem from combining robust state tracking with counting-like accumulation.

Our contributions are: **(i) A comparison of leading subquadratic operators on tasks with complex dependencies.** We provide the first head-to-head comparison of xLSTM, Mamba-2, and Gated DeltaNet across settings that go beyond standard English-web pre-training. xLSTM backbones lead across most settings in empirical evaluation. **(ii) A unified formulation of xLSTM, Mamba-2, and Gated DeltaNet that yields a hypothesis for the empirical differences.** We express the three backbones within a single framework, bridging their original state-space model and linear-attention notations. The formulation predicts that the architectures differ primarily on two primitives: accumulation and finite-state tracking. **(iii) A validation of this hypothesis on synthetic tasks.** We empirically test the hypothesis on controlled length-generalization tasks for counting and state tracking.

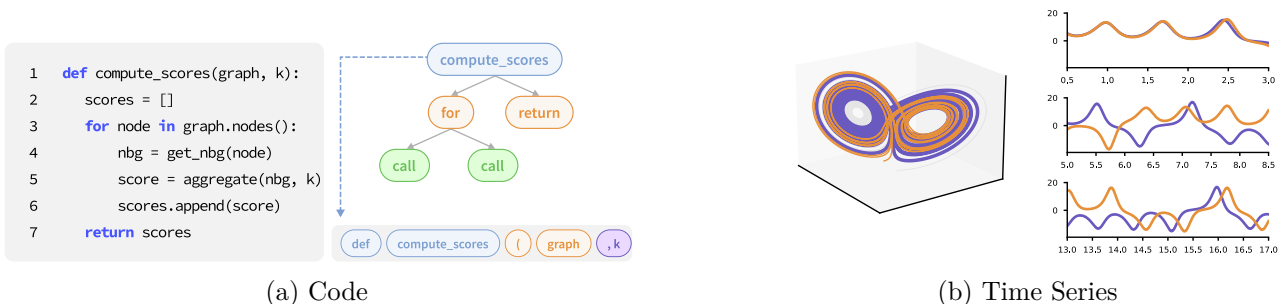


Figure 1: **Tasks with complex dependencies.** Code (a) carries dependencies in formal structure: syntax trees, call graphs, variable bindings. Time series (b) carries them in partially observed dynamics: trajectories of complex systems (here, a Lorenz attractor) whose future depends on unobserved states over history. Both are representative of complex dependencies where modeling requires tracking many interacting states across long contexts.

¹The xLSTM family combines matrix-state linear-attention layers, denoted xLSTM[1:0] or mLSTM, with recurrent layers, denoted xLSTM[0:1] or sLSTM; xLSTM[m:s] denotes the ratio of these two components.

2 Experiments with Complex Dependencies

We begin with the empirical comparison. The goal of this section is not to explain why the architectures differ, but to establish the practical pattern that the rest of the paper explains. We find that across code-focused language-model pre-training (Section 2.1), code-focused Transformer distillation (Section 2.2), and time-series foundation-model pre-training (Section 2.3), xLSTM-family backbones outperform the other subquadratic operators in nearly all comparisons. The strongest gains appear on complex structured tasks, while broad reasoning and commonsense benchmarks show the same direction with smaller margins. This consistent empirical advantage motivates our architectural analysis in Section 3, followed by controlled synthetic tasks in Section 4.

2.1 Code-focused Language-Model Pre-training

We first compare subquadratic backbones in code-focused language-model pre-training. Code is a complex language setting because it combines natural-language-like token distributions with formal syntax, variable binding, and executable structure. We therefore use code generation as the primary metric in this subsection and report broad reasoning and commonsense tasks as a secondary check.

Experimental setup. We pretrain 400M-parameter inter-layer hybrid language models with `lm-engine` (Mishra, 2024), into which we integrate the xLSTM backbone alongside the existing Attention, Mamba-2, and Gated DeltaNet operators. Here, “inter-layer hybrid” means that most layers use the tested subquadratic sequence operator, while a small number of layers remain standard self-attention layers. We compare Gated DeltaNet, Mamba-2, and xLSTM [7:1]². All three models use 24 layers in total and keep three self-attention layers, matching the small fraction of self-attention used in contemporary hybrid architectures (Team, 2025a; Ren et al., 2025; NVIDIA, 2025; Merrill et al., 2026b; Team, 2025b). We train under three data configurations: Nemotron-CC-Code-v1 (NVIDIA, 2025) for 20B as well as 100B tokens, and a Nemotron-CC-Code-v1 + FineWeb-Edu mixture for 20B tokens. We evaluate code generation with HumanEval pass@ k for $k \in \{2, 8, 16, 64\}$, and report reasoning and commonsense accuracy on HellaSwag, PIQA, ARC-Easy, ARC-Challenge, and WinoGrande. Further details on the setup are provided in Appendix F.1.

xLSTM [7:1] consistently leads on code generation. As shown in Figure 2, xLSTM [7:1] leads at every pass@ k and in every training configuration. At pass@64, it improves over the next-best backbone by 1.43 points at 20B code tokens, 0.90 points at 100B code tokens, and 1.81 points on the mixed code-and-FineWeb-Edu corpus. The runner-up is consistently Gated DeltaNet when trained on code-only data corpus. Full results are reported in Appendix B Tables 3, 4, and 5.

xLSTM [7:1] keeps a smaller aggregate lead on reasoning and commonsense. Across the five reasoning and commonsense benchmarks, xLSTM [7:1] has the best aggregate score in all three training configurations. The margins are smaller than on HumanEval: it leads the closest non-xLSTM backbone by under 0.1 points at 20B and 100B code tokens, and by roughly half a point on the Nemotron-CC-Code-v1 + FineWeb-Edu mix. Thus, the broad benchmarks agree with the code-generation ordering, but they make the xLSTM advantage less visible. The full per-task results are reported in Appendix B Tables 6, 7, and 8.

Discussion. The pre-training results show a consistent advantage for xLSTM [7:1] among the compared backbones. It leads to code generation in every training configuration and at every reported sampling budget. It also has the best aggregate reasoning and commonsense score, although margins are smaller. This supports the role of complex structured tasks in our evaluation: they reveal the same ordering as broad benchmarks, but with clearer separation between subquadratic backbones.

²Unlike the pure xLSTM[m:s] convention, the hybrid pre-training blocks also contain softmax attention. We fold these into the first index, so xLSTM[7:1] reads as 7 non-recurrent layers (6 mLSTM + 1 self-attention) to 1 recurrent layer.

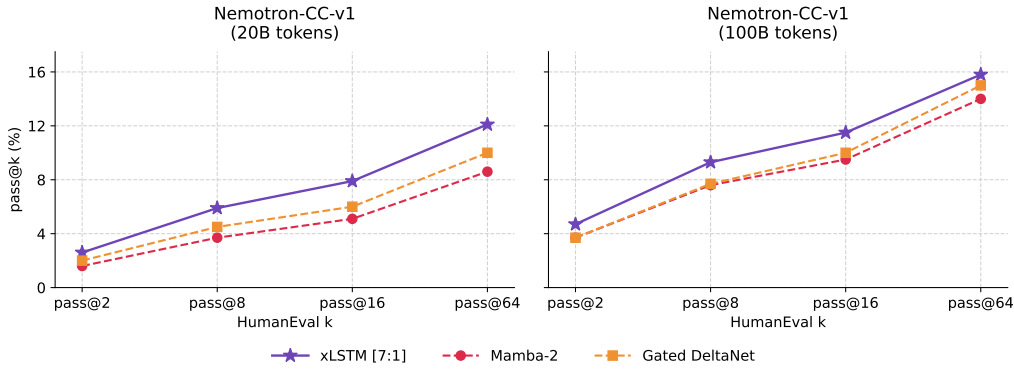


Figure 2: **HumanEval pass@k after code-focused pre-training.** Results for 400M-parameter hybrid language models trained under the matched pre-training recipe on two data configurations: Nemotron-CC-Code-v1 for 20B tokens, Nemotron-CC-Code-v1 for 100B tokens. For 100B tokens, the gap between the different subquadratic backbones shrinks.

Section 2.2 and Section 2.3 test whether xLSTM’s advantage persists in distillation and time-series foundation-model pre-training.

2.2 Code-focused Transformer Distillation into Subquadratic Students

Having compared subquadratic backbones in code-focused pre-training, we next ask whether these operators remain effective when initialized from a strong attention-based teacher. Linearization, a form of knowledge distillation (Hinton et al., 2015; Mercat et al., 2024), converts an open-weight Transformer teacher into a subquadratic student and avoids a separate from-scratch pre-training run for each candidate operator. We use the recipe of Hauzenberger et al. (2026), which combines a sliding-window-attention scaffold with attention sinks, hidden-state alignment, and sparse top- k knowledge distillation. Prior linearization work typically fixes the target operator family, such as linear/sliding-window attention, Mamba-style state-space mixers, RWKV, or gated recurrent structures (Zhang et al., 2025; Bick et al., 2024, 2025; Wang et al., 2024; Goldstein et al., 2025; Lan et al., 2025). We instead compare xLSTM[1:0] and Gated DeltaNet as plug-in matrix-state replacements under the same teacher, data, initialization scheme, and optimization recipe. For code distillation, we additionally evaluate Gated DeltaNet $[-1, 1]$, which uses the negative-eigenvalue parameterization of Grazzi et al. (2025).

Experimental setup. Our teacher is Qwen3-4B-Instruct (Team, 2025c). The student keeps the teacher’s width, depth, and tokenizer. We replace every multi-head-attention block with an intra-layer hybrid block: the tested linear-attention operator runs in parallel with sliding-window attention of window size 512 and four sink tokens (Xiao et al., 2024; Beltagy et al., 2020), and a learned data-dependent gate fuses the two paths. The linear-attention branch inherits the teacher’s q , k , and v projection weights at initialization. We follow the two-stage protocol of Hauzenberger et al. (2026). Stage I aligns per-layer student outputs with the teacher’s attention outputs under an MSE loss. Stage II minimizes $0.9 \text{ CE} + 0.1 \text{ KL}$ with top- $k = 256$ sparse teacher distribution. Sequence length is 4,096, and we train for 10,000 stage-II optimization steps. Code distillation uses Nemotron-Pretraining-Code-v2 (NVIDIA, 2025). Because the distilled students keep the 4B teacher architecture, we use a harder code-generation suite than in Section 2.1: HumanEval, HumanEval+, MBPP, and MBPP+. Appendix F.2 gives the full implementation details.

xLSTM[1:0] and Gated DeltaNet are the plug-in comparison. The distillation setup supports linear-attention replacements that expose query, key, and value projections, admit chunkwise-parallel kernels, and reuse the teacher’s attention projections at initialization. Both xLSTM[1:0] (mLSTM; Beck et al., 2024) and Gated DeltaNet satisfy these constraints and slot in without changing the surrounding hybrid block. Gated DeltaNet also provides the stricter non-xLSTM comparison

Table 1: **Code distillation results at pass@1.** Students are distilled from Qwen3-4B-Instruct. xLSTM[1:0] leads on three of four benchmarks and on average, while the default Gated DeltaNet performs better on MBPP+. Gated DeltaNet $[-1, 1]$ improves over the default Gated DeltaNet on HumanEval and HumanEval+ but not on MBPP and MBPP+. Higher is better; the best student result per column is shown in **bold**.

Student	HumanEval \uparrow	HumanEval+ \uparrow	MBPP \uparrow	MBPP+ \uparrow	Avg. \uparrow
Qwen3-4B-Instruct (teacher)	0.914	0.835	0.708	0.847	0.826
xLSTM[1:0]	0.831	0.764	0.689	0.788	0.768
Gated DeltaNet	0.802	0.739	0.677	0.802	0.755
Gated DeltaNet $[-1, 1]$	0.813	0.745	0.671	0.796	0.756

for code distillation, since in the directly related code-only pre-training setting, it is the strongest non-xLSTM backbone on HumanEval at both 20B and 100B tokens (Section 2.1; Appendix Tables 3 and 4). In contrast, xLSTM[0:1] is sequential and has no query-key-value analogue to initialize from the teacher, while Mamba-2 ties its input and forget gates through parameters that do not map directly to teacher attention weights. We therefore use this experiment as a controlled comparison between plug-in matrix-state operators, not as a test of the full xLSTM hybrid family.³ We report Gated DeltaNet with its default parameterization and, for code, the Gated DeltaNet $[-1, 1]$ variant (see Appendix F.2).

xLSTM[1:0] gives the stronger code student on average. Across the four code benchmarks at pass@1, xLSTM[1:0] matches or exceeds default Gated DeltaNet on three metrics and trails only on MBPP+ by 0.014 (Table 1). The negative-eigenvalue variant improves Gated DeltaNet on HumanEval and HumanEval+, but trails the default variant on MBPP and MBPP+. The average across HumanEval, HumanEval+, MBPP, and MBPP+ is 0.755 for default Gated DeltaNet, 0.756 for Gated DeltaNet $[-1, 1]$, and 0.768 for xLSTM[1:0]. The full HumanEval and HumanEval+ pass@ k spread in Appendix C.1 shows that xLSTM[1:0] remains strongest across sampling budgets.

Discussion. The distillation experiment complements code-focused pre-training by testing the same operator comparison inside a Transformer-linearization pipeline. Under a fixed teacher, data, initialization scheme, and optimization recipe, xLSTM[1:0] gives the stronger code student on average. This shows that the xLSTM advantage in code-focused settings does not rely only on the recurrent layers used in xLSTM inter-layer hybrids (Section 2.1): the linear-attention component is already a strong plug-in operator. Appendix C.2 reports the corresponding math-distillation results, where xLSTM[1:0] also leads the aggregate while Gated DeltaNet remains slightly stronger on MATH-500. Together, the code and math results support xLSTM[1:0] as an effective matrix-state replacement in Transformer distillation to subquadratic architectures.

2.3 Time-series Foundation-Model Pre-training

After code-focused pre-training and distillation, we ask whether the same architectural comparison also holds outside these tasks. Time Series Foundation Models (TSFM) have so far been built primarily on Transformer backbones (Ansari et al., 2024; Woo et al., 2024; Das et al., 2024; Cohen et al., 2024), with subquadratic backbones emerging as recent alternatives. TiRex (Auer et al., 2025) demonstrates that an xLSTM-based TSFM is competitive, TempoPFN (Moroshan et al., 2025) adopts Gated DeltaProduct (Siems et al., 2025), a Gated DeltaNet variant, and FlowState (Graf et al., 2025) uses the S5 state-space variant. These works establish strong individual designs, but they do not compare subquadratic backbone families under a matched setting. Time series, therefore, provides a

³The distillation setup can extend to xLSTM[0:1] or other xLSTM[$m:s$] variants, and Mamba-2, but these require additional initialization and architecture choices and would no longer isolate the plug-in matrix-state comparison studied here.

complementary complex-task setting with continuous values, heterogeneous domains and frequencies, and forecasting horizons that require models to use information from long histories.

Experimental setup. We use the time-series pre-training protocol of Auer et al. (2025): the same corpus, patching scheme, optimizer, and forecasting head are shared across all models, while only the sequence mixer changes. Thus, the comparison isolates the backbone choice within a fixed forecasting pipeline. We compare Mamba-2, Gated DeltaNet, and xLSTM [3 : 1]. Models are trained at five parameter scales: 1M, 4M, 10M, 40M, and 80M parameters, with width and depth chosen to match the parameter count in each setting. This range is small compared with contemporary language models, but it is a practical scale range for TSFMs; for example, both TiRex and FlowState report strong forecasting performance in the 20-35M parameter range (Auer et al., 2025; Graf et al., 2025). We evaluate zero-shot on GIFT-Eval (Aksu et al., 2024), a heterogeneous forecasting benchmark spanning multiple domains and frequencies, and report Mean Absolute Scaled Error (MASE) and Continuous Ranked Probability Score (CRPS) aggregated by geometric mean. Appendix F.3 gives the implementation details, and Appendix D reports the full numerical results.

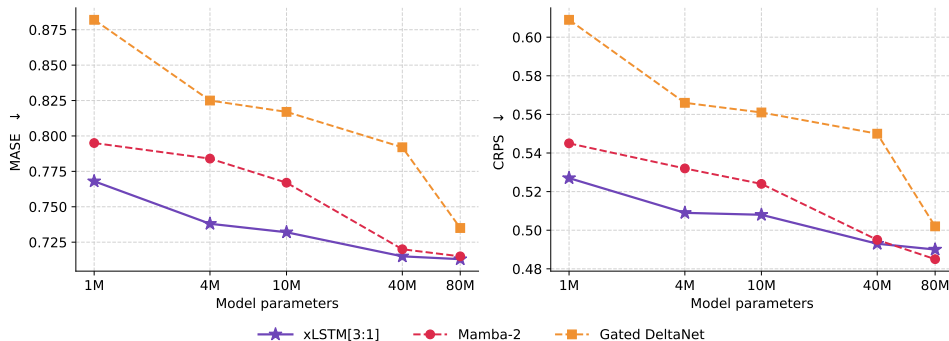


Figure 3: **GIFT-Eval performance of TSFM over five parameter scales.** MASE and CRPS scores (lower is better) for matched training recipe. xLSTM architectures provide the best scores, with the gap narrowing as the parameter scale grows.

xLSTM [3 : 1] leads from 1M to 40M parameters. Figure 3 sweep shows a clear small-to-mid-scale advantage for xLSTM [3 : 1]. It achieves the best MASE and CRPS at every scale from 1M to 40M parameters. The separation is most visible at small and mid scales. At 10M parameters, for example, xLSTM [3 : 1] reaches 0.733 MASE and 0.508 CRPS, compared with 0.767 and 0.525 for the next-best model (Mamba-2). At 80M parameters, the models nearly converge: xLSTM [3 : 1] and Mamba-2 are on par on MASE, while Mamba-2 slightly leads on CRPS by 0.005. The full values are reported in Appendix D, Table 12.

Discussion. The time-series results extend the practical comparison beyond language. Under a matched TSFM recipe, xLSTM [3 : 1] is the strongest backbone from 1M to 40M parameters, while the gap narrows at 80M. Together with Sections 2.1 and 2.2, these results show a consistent empirical pattern: xLSTM-family backbones outperform the competing subquadratic operators in nearly all matched practical comparisons. The few exceptions are narrow: Gated DeltaNet leads MBPP+ in distillation, and Mamba-2 leads CRPS by 0.005 at 80M parameters. The next sections hypothesize where this advantage comes from. Section 3 analyzes the memory dynamics of the architectures, and Section 4 tests the resulting hypotheses on controlled counting and state-tracking tasks.

3 Analysis of Leading Subquadratic Attention Architectures

In order to better understand the empirical differences between the architectures, we take a closer look at the underlying attention mechanisms. Concretely, we express xLSTM, Mamba-2, and Gated

DeltaNet in terms of linear attention with a gating mechanism using a common notation.

Attention mechanisms (Vaswani et al., 2017; Bahdanau et al., 2015) are specified in terms of *query*, *key*, and *value* matrices,

$$\mathbf{Q} = \mathbf{X}\mathbf{W}_q^\top \quad \mathbf{K} = \mathbf{X}\mathbf{W}_k^\top \quad \mathbf{V} = \mathbf{X}\mathbf{W}_v^\top,$$

where $\mathbf{W}_{\{q,k\}} \in \mathbb{R}^{D_{qk} \times D}$, $\mathbf{W}_v \in \mathbb{R}^{D_v \times D}$ represent learnable parameters of the affine projections, and $\mathbf{X} \in \mathbb{R}^{T \times D}$ is a sequence of inputs. With these matrices, the regular, causal softmax attention can be written as $\text{softmax}(\mathbf{Q}\mathbf{K}^\top \odot \mathbf{M})\mathbf{V}$, where $\mathbf{M} \in \{-\infty, 1\}^{T \times T}$ is a causal masking matrix, such that $m_{ij} = 1$ if $i \geq j$ and $-\infty$ otherwise.

Linear attention (Katharopoulos et al., 2020) is a basic subquadratic attention variant that does away with the softmax in regular attention. This enables a recurrent formulation for single-head linear attention that exposes an explicit matrix state, $\mathbf{C} \in \mathbb{R}^{D_{qk} \times D_v}$:

$$\mathbf{H} = \frac{(\mathbf{Q}\mathbf{K}^\top \odot \mathbf{M})\mathbf{V}}{(|\mathbf{Q}\mathbf{K}^\top| \odot \mathbf{M})\mathbf{1}} \quad (\text{parallel})$$

$$\mathbf{h}_t = \frac{\mathbf{q}_t \mathbf{C}_t}{|\mathbf{q}_t \mathbf{n}_t|} \quad \mathbf{C}_t = \mathbf{C}_{t-1} + \mathbf{k}_t \otimes \mathbf{v}_t \quad \mathbf{n}_t = \mathbf{n}_{t-1} + \mathbf{k}_t, \quad (\text{recurrent})$$

where division is element-wise, \otimes denotes the outer product, $1 \leq t \leq T$, $\mathbf{C}_0 = \mathbf{0}$, $\mathbf{n}_0 = \mathbf{0}$ and $\mathbf{M} \in \{0, 1\}^{T \times T}$ is a causal masking matrix. Note that the explicit normalization, inspired by the normalization inside the softmax function (Katharopoulos et al., 2020), is commonly ignored in practice (cf. Yang et al., 2024a; Yang and Zhang, 2026). Instead, this normalization is implemented by normalization layers (e.g. Ba et al., 2016; Wu and He, 2018). To ease notation, we omit the explicit normalization throughout this work, unless necessary.

The recurrent formulation of linear attention is what enables its subquadratic nature, i.e., $\mathcal{O}(T)$ instead of $\mathcal{O}(T^2)$ for regular attention and the parallel formulation. However, the recurrent formulation can not make use of hardware that is optimized for matrix multiplications, making it slow in practice. As a result, practical implementations use the intermediate chunk-wise formulation (Hua et al., 2022):

$$\begin{aligned} \mathbf{H}_{[n]} &= (\mathbf{Q}_{[n]}\mathbf{K}_{[n]}^\top \odot \mathbf{M})\mathbf{V}_{[n]} + \mathbf{Q}_{[n]}\mathbf{C}_{(n-1)C} \\ \mathbf{C}_{nC} &= \mathbf{C}_{(n-1)C} + \mathbf{K}_{[n]}^\top \mathbf{V}_{[n]}, \end{aligned} \quad (\text{chunkwise})$$

where the C time steps within each chunk are processed in parallel, while the explicit state is used to connect the different chunks sequentially. This enables linear complexity while allowing efficient usage of modern hardware. Here, $1 \leq n \leq \lceil T/C \rceil$, $\mathbf{X}_{[n]}$ is a short-hand for $\mathbf{X}_{((n-1)C+1:nC)}$, i.e. the chunk for all time-steps t with $(n-1)C+1 \leq t \leq nC$ (cf. Yang et al., 2024a), and, with slight abuse of notation, $\mathbf{M} \in \{0, 1\}^{C \times C}$ represents the causal mask for a single chunk. Note that the chunk-wise formulation reduces to the (unnormalized) parallel and recurrent formulations if $C = T$ and $C = 1$, respectively.

xLSTM (Beck et al., 2024) is a modern version of LSTM (Hochreiter and Schmidhuber, 1997; Gers et al., 1999). It consists of a linear attention component, called mLSTM or xLSTM[1:0], and a non-linear recurrent component, called sLSTM or xLSTM[0:1]. These components can be combined to form the xLSTM[$m:s$] architecture, where m and s represent the number of linear attention and recurrent layers, respectively. The recurrence of a single xLSTM[0:1] head is given by:

$$\begin{aligned} \mathbf{v}_t &= \tanh(\mathbf{W}_v \mathbf{x}_t + \mathbf{R}_v \mathbf{h}_{t-1}) & \mathbf{q}_t &= \mathbf{e}_1 & \mathbf{k}_t &= \mathbf{1} \\ \mathbf{i}_t &= \exp(\mathbf{W}_i \mathbf{x}_t + \mathbf{R}_i \mathbf{h}_{t-1}) & \mathbf{f}_t &= \sigma(\mathbf{W}_f \mathbf{x}_t + \mathbf{R}_f \mathbf{h}_{t-1}) \\ \mathbf{c}_t &= \text{diag}(\mathbf{f}_t) \mathbf{c}_{t-1} + \text{diag}(\mathbf{i}_t) \mathbf{v}_t & \mathbf{n}_t &= \text{diag}(\mathbf{f}_t) \mathbf{n}_{t-1} + \mathbf{i}_t \\ \mathbf{h}_t &= \frac{\mathbf{c}_t}{\mathbf{n}_t}, \end{aligned} \quad (1)$$

where the division is element-wise, and $\mathbf{W}_{\{i,f,v\}}$ and $\mathbf{R}_{\{i,f,v\}} \in \mathbb{R}^{D \times D}$ are learnable parameters for the input and forget gate, as well as the state update. Note that we redefine the keys, queries, and values and explicitly model the normalizer state because the xLSTM[0:1] does not perfectly align with the linear attention paradigm. The linear attention mechanism of a single xLSTM[1:0] head, on the other hand, can be expressed using the following recurrence:

$$\begin{aligned} i_t &= \exp(\mathbf{w}_i \mathbf{x}_t) & f_t &= \sigma(\mathbf{w}_f \mathbf{x}_t) \\ \mathbf{h}_t &= \mathbf{q}_t \mathbf{C}_t & \mathbf{C}_t &= f_t \mathbf{C}_{t-1} + i_t \mathbf{k}_t \otimes \mathbf{v}_t. \end{aligned} \quad (2)$$

Here, $\mathbf{w}_{\{i,f\}}$ are the learnable parameters for the input and forget, and we assume biases are implicit. One of the key differences between xLSTM and LSTM is the exponential input gate. When normalized correctly, this input gate behaves like a softmax over time, allowing the model to down-weight, or overwrite, previous values when the current value is more important. The main difference between xLSTM[0:1] and xLSTM[1:0] is the use of recurrent weights to incorporate the previous state. This recurrence enables state-tracking capabilities similar to those of other recurrent networks (Merrill, 2019). Note that we ignore the output gate in these formulations, as it is typically implemented using a SwiGLU (Shazeer, 2020), which has become a common component in the block-wrappers around the core attention mechanism (Gu and Dao, 2024; Yang et al., 2024b; Beck et al., 2024).

Mamba-2 (Dao and Gu, 2024) is a linear attention variant derived from state-space models (e.g. Gu et al., 2022; Gupta et al., 2022; Gu and Dao, 2024). The recurrent formulation for a single head in the attention mechanism of Mamba-2 can be expressed as follows:

$$\begin{aligned} i_t &= \text{softplus}(\mathbf{w}_\Delta \mathbf{x}_t) & f_t &= (1 - \sigma(\mathbf{w}_\Delta \mathbf{x}_t))^a \\ \mathbf{h}_t &= \mathbf{q}_t \mathbf{C}_t & \mathbf{C}_t &= f_t \mathbf{C}_{t-1} + i_t \mathbf{k}_t \otimes \mathbf{v}_t. \end{aligned} \quad (3)$$

Here, \mathbf{w}_Δ are the learnable parameters for computing the sample time in the zero-order hold discretisation (Gupta et al., 2022; Gu and Dao, 2024), and $a \in \mathbb{R}_{\geq 0}$ is a non-negative learned parameter to construct the 1-SS transition matrix. As a result, Mamba-2 can be interpreted as an xLSTM[1:0] with tied input and forget gates, making it similar to a Gated Recurrent Unit (GRU) (Cho et al., 2014; Dao and Gu, 2024). Because GRUs are known to have issues with counting (e.g. Weiss et al., 2018), we expect Mamba-2 to have similar limitations.

Gated DeltaNet (Yang et al., 2024b) is practically a combination of the fast-weight mechanism of Delta-Nets (Schlag et al., 2021) and the 1-SS transition dynamics of Mamba-2 (Dao and Gu, 2024). The recurrence of this linear attention variant can be written as:

$$\begin{aligned} i_t &= \sigma(\mathbf{w}_\beta \mathbf{x}_t) & f_t &= (1 - \sigma(\mathbf{w}_\alpha \mathbf{x}_t))^a \\ \mathbf{h}_t &= \frac{\mathbf{q}_t}{\|\mathbf{q}_t\|} \mathbf{C}_t & \mathbf{C}_t &= f_t \left(\mathbf{I} - i_t \frac{\mathbf{k}_t \otimes \mathbf{k}_t}{\|\mathbf{k}_t\|^2} \right) \mathbf{C}_{t-1} + i_t \frac{\mathbf{k}_t}{\|\mathbf{k}_t\|} \otimes \mathbf{v}_t, \end{aligned} \quad (4)$$

where \mathbf{w}_α and \mathbf{w}_β are the learnable parameters for the gating and write-strength (Schlag et al., 2021), respectively, and $a \in \mathbb{R}_{\geq 0}$ is a non-negative learned parameter from Mamba-2. We note that Gated DeltaNet can be interpreted as an xLSTM[1:0] with an additional state transformation. The matrix $\mathbf{I} - \frac{\mathbf{k}_t \otimes \mathbf{k}_t}{\|\mathbf{k}_t\|^2}$ is an orthogonal projection onto the null-space of \mathbf{k}_t . This means that the additional transformation removes all components in the direction of \mathbf{k}_t from the state when $i_t = 1$. E.g., when $\mathbf{k}_t = \mathbf{k}_s$ for some $s < t$, the old value, \mathbf{v}_s , will be removed from the state matrix and replaced by the new value, \mathbf{v}_t . Because old values are always overwritten, Gated DeltaNets are also expected to have problems with counting.

All linear attention variants exhibit very similar gating mechanisms. Concretely, each of these models can be written in terms of input and forget gates, similar to LSTM. Whereas xLSTM and Gated DeltaNets have independent gates, the input and forget gate in Mamba-2 are tied and therefore expected to be less expressive. Another key difference lies in the overwriting mechanism of the input

gate. Mamba-2 has limited capabilities to correct weights in previous time-steps due to its linear-like input gate. Gated DeltaNet explicitly overwrites old values in the state, making it better suited for retrieval tasks (Yang et al., 2024b), but can be problematic for counting. The xLSTM architecture enables the most flexible weighting correction that allows down-weighting old values by means of the softmax-like input gate.

We attribute this advantage to xLSTM’s ability to solve counting and state tracking.

Recent theory points to two capabilities that sequence models often fail to combine: accumulation over unbounded lengths and finite-state tracking (Weiss et al., 2018; Merrill et al., 2026a). Mamba-style state-space models and (Gated) DeltaNets inherit the TC^0 ceiling of Transformers and cannot solve hard state-tracking problems such as permutation composition (Merrill et al., 2024; Grazzi et al., 2025); related limitations appear in code modeling (Siems et al., 2026). However, Grazzi et al. (2025) points out that this can be alleviated by enabling negative eigenvalues in the state-transition matrix. Concretely, mapping the forget gate to values in $[-1, 1]$ instead of $[0, 1]$ should improve state-tracking significantly. Within xLSTM, the matrix-state update provides a natural mechanism for accumulation, while the nonlinear recurrent component can support structured state updates. This makes mixed xLSTM $[m:s]$ architectures a plausible way to combine accumulation with state tracking in a scalable backbone. We therefore interpret the strong performance of xLSTM on complex domains such as code and time series as evidence that these capabilities are useful in combination, rather than as a consequence of either mechanism in isolation.

4 Experiments on Accumulation and State Tracking

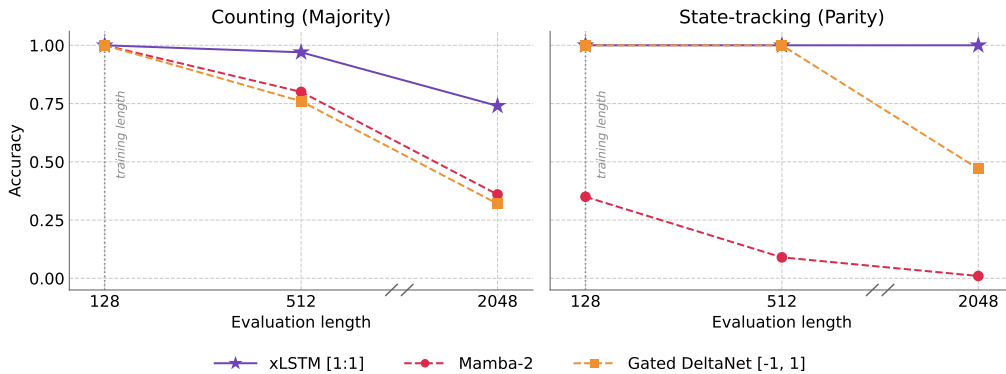


Figure 4: **Length generalization on accumulation and state-tracking.** Two representative tasks (Majority counting on the left, parity on the right) on which contemporary subquadratic designs diverge. Models are trained at length 128 (dotted line) and evaluated at 128, 512, and 2048; the break on the x-axis marks the $4\times$ jump from 512 to 2048. xLSTM[1:1] is the only configuration that length-generalizes on both tasks: it achieves the highest counting accuracy at every length and solves parity perfectly throughout. Gated DeltaNet with the negative-eigenvalue parameterization of Grazzi et al. (2025) solves parity in-distribution but drops to 0.47 at length 2048; Mamba-2 never solves either.

Experimental Setup. Each model is trained at sequence length 128 and evaluated at lengths 128, 512, and 2048, covering a $4\times$ and $16\times$ extrapolation step. The counting tasks are $A^n B^n$, $A^n B^n C^n$, and Majority; the state-tracking tasks are Parity, Modular Arithmetic (\mathbb{Z}_5), and word-problem evaluation in the symmetric group S_3 . We compare Mamba-2, Gated DeltaNet with the default non-negative eigenvalue parameterization (Gated DeltaNet) and with the negative-eigenvalue parameterization of Grazzi et al. (2025) (Gated DeltaNet $[-1, 1]$), xLSTM[1:0] and xLSTM[1:1]. All models are trained under identical setups; full details are in Appendix F.4.

Only xLSTM combines both accumulation and state tracking. Table 13 in Appendix E reports accuracy at each evaluation length, and Figure 4 matches the architectural predictions above. Mamba-2 collapses on every task: $A^n B^n$ accuracy drops from 1.000 at length 128 to 0.241 at 2048, and Parity accuracy never exceeds 0.352 even in-distribution. Default Gated DeltaNet solves the easiest counting variant at moderate length, but degrades to 0.268 on Majority at 2048 and never solves any state-tracking task. Gated DeltaNet $[-1, 1]$ recovers Parity and S_3 in-distribution (1.000 at length 128). Still, length-generalisation on these tasks is only partial: Parity drops to 0.472 at length 2048 and S_3 to 0.667, and the parameterization does not improve modular arithmetic (0.452 at length 2048). xLSTM[1:0] length-generalises on every counting task (0.892 on $A^n B^n$, 0.932 on $A^n B^n C^n$, 0.763 on Majority at length 2048) but, as expected for a linear-attention block, fails on every state-tracking task. The hybrid xLSTM[1:1] is the best balanced configuration rather than the best model on every task. It is exact on all three state-tracking tasks and retains useful counting extrapolation, but it trails xLSTM[1:0] on the hardest long counting tasks.

Discussion. The synthetic results separate the two primitives. The xLSTM [1:0] is the strongest counting model, consistent with the accumulation mechanism introduced above, but fails on state-tracking tasks. Conversely, adding the recurrent xLSTM [0:1] component in xLSTM [1:1] yields perfect state tracking at all tested lengths, while preserving useful but weaker counting extrapolation. Gated DeltaNet exhibits the expected tradeoff: the default parameterization does not solve state tracking, while the negative-eigenvalue variant improves state tracking but does not consistently extrapolate. These results motivate m-heavy xLSTM $[m:s]$ models in practical settings, such as xLSTM[7:1] for language pretraining and xLSTM[3:1] for time series: they retain the efficient accumulation block as the dominant component while adding a smaller number of recurrent layers for state tracking.

5 Conclusion

We have conducted the first comparison of xLSTM, Mamba-2, and Gated DeltaNet across more complex data domains. Our experiments show that xLSTM backbones outperform other subquadratic operators in nearly all comparisons across all studied settings. These empirical results motivated our analysis of why xLSTM performs better under the proposed settings. To explain xLSTM’s advantage on complex tasks, we derived a common formulation that makes the architectures directly comparable at the level of memory dynamics. Our formulation shows how gates, normalization, and overwriting mechanisms shape two primitive capabilities: *accumulation* and *finite-state tracking*. We have found that Mamba-2 couples writing and forgetting through tied gates, while Gated DeltaNet adds explicit overwriting, which helps replacement-style memory updates but can interfere with accumulation. In contrast, xLSTM separates matrix-state linear attention from recurrent state updates, giving it a direct way to combine accumulation, state tracking, and flexible memory correction.

Limitations and Future Work. First, our code-focused language modeling is conducted at a 400M-parameter scale, and our distillation pipeline uses a single teacher; only the time-series experiments include a scaling sweep. Extending the comparison to larger model scales, additional teachers, and further data domains is a natural next step. Second, we focus on recent leading subquadratic architectures and exclude families already compared in Beck et al. (2024); a broader operator survey under our unified formulation would further sharpen the picture.

Acknowledgments

This work was supported by the Austrian Science Fund (FWF) 10.55776/COE12 and the European Union’s Horizon Europe research and innovation program under grant agreement number 101214398 (ELLIOT). The ELLIS Unit Linz, the LIT AI Lab, and the Institute for Machine Learning are supported by the Federal State of Upper Austria. We acknowledge the EuroHPC Joint Undertaking for awarding us access to Leonardo at CINECA, Italy.

References

- Taha Aksu, Gerald Woo, Juncheng Liu, Xu Liu, Chenghao Liu, Silvio Savarese, Caiming Xiong, and Doyen Sahoo. GIFT-Eval: A Benchmark for General Time Series Forecasting Model Evaluation. In *NeurIPS Workshop on Time Series in the Age of Large Models*, 2024. URL <https://openreview.net/forum?id=Z2cM00ANFX¬eId=Z2cM00ANFX>.
- Abdul Fatir Ansari, Lorenzo Stella, Ali Caner Turkmen, Xiyuan Zhang, Pedro Mercado, Huibin Shen, Oleksandr Shchur, Syama Sundar Rangapuram, Sebastian Pineda Arango, Shubham Kapoor, Jasper Zschiegner, Danielle C. Maddix, Hao Wang, Michael W. Mahoney, Kari Torkkola, Andrew Gordon Wilson, Michael Bohlke-Schneider, and Bernie Wang. Chronos: Learning the Language of Time Series. *Transactions on Machine Learning Research*, 2024. ISSN 2835-8856. URL <https://openreview.net/forum?id=gerNCVqqtR>.
- Andreas Auer, Patrick Podest, Daniel Klotz, Sebastian Böck, Günter Klambauer, and Sepp Hochreiter. TiRex: Zero-Shot Forecasting Across Long and Short Horizons with Enhanced In-Context Learning. In *Advances in Neural Information Processing Systems*, volume 38, pages 57529–57580. Curran Associates, Inc., 2025. URL https://proceedings.neurips.cc/paper_files/paper/2025/hash/5356603f9c47399adfd372f77a677057-Abstract-Conference.html.
- Jimmy Lei Ba, Jamie Ryan Kiros, and Geoffrey E. Hinton. Layer Normalization, 2016. URL <http://arxiv.org/abs/1607.06450>. arXiv:1607.06450 [stat].
- Dzmitry Bahdanau, KyungHyun Cho, and Yoshua Bengio. Neural machine translation by jointly learning to align and translate. *International Conference on Learning Representations*, 2015.
- Maximilian Beck, Korbinian Pöppel, Markus Spanring, Andreas Auer, Oleksandra Prudnikova, Michael Kopp, Günter Klambauer, Johannes Brandstetter, and Sepp Hochreiter. xLSTM: Extended Long Short-Term Memory. In *Advances in Neural Information Processing Systems*, volume 37, pages 107547–107603, Vancouver, BC, Canada, 2024. Curran Associates, Inc. doi: 10.52202/079017-3417. URL https://proceedings.neurips.cc/paper_files/paper/2024/hash/c2ce2f2701c10a2b2f2ea0bfa43cfaa3-Abstract-Conference.html.
- Maximilian Beck, Korbinian Pöppel, Phillip Lippe, Richard Kurle, Patrick M. Blies, Günter Klambauer, Sebastian Böck, and Sepp Hochreiter. xLSTM 7B: A Recurrent LLM for Fast and Efficient Inference. In *Proceedings of the 42nd International Conference on Machine Learning*, volume 267, pages 3335–3357. PMLR, 2025. URL <https://proceedings.mlr.press/v267/beck25b.html>.
- Maximilian Beck, Kajetan Schweighofer, Sebastian Böck, Sebastian Lehner, and Sepp Hochreiter. xLSTM Scaling Laws: Competitive Performance with Linear Time-Complexity. In *International Conference on Learning Representations*, volume 14. OpenReview, 2026. URL <https://openreview.net/forum?id=bpbU549sSg>.
- Iz Beltagy, Matthew E. Peters, and Arman Cohan. Longformer: The Long-Document Transformer, 2020. URL <http://arxiv.org/abs/2004.05150>. arXiv:2004.05150 [cs].
- Aviv Bick, Kevin Y. Li, Eric P. Xing, J. Z. Kolter, and Albert Gu. Transformers to SSMS: Distilling Quadratic Knowledge to Subquadratic Models. In *Advances in Neural Information Processing Systems*, volume 37, pages 31788–31812, Vancouver, BC, Canada, 2024. Curran Associates, Inc. doi: 10.52202/079017-0999. URL https://proceedings.neurips.cc/paper_files/paper/2024/hash/3848fef259495bfd04d60cdc5c1b4db7-Abstract-Conference.html.
- Aviv Bick, Tobias Katsch, Nimit Sharad Sohoni, Arjun D. Desai, and Albert Gu. Llama: Scaling Distilled Recurrent Models for Efficient Language Processing. In *Conference on Language Modeling*, volume 1, Singapore, Singapore, 2025. OpenReview. URL <https://openreview.net/forum?id=uciWntM6iv>.
- Sidney Black, Stella Biderman, Eric Hallahan, Quentin Anthony, Leo Gao, Laurence Golding, Horace He, Connor Leahy, Kyle McDonell, Jason Phang, Michael Pieler, Usvsn Sai Prashanth, Shivanshu Purohit, Laria Reynolds, Jonathan Tow, Ben Wang, and Samuel Weinbach. GPT-NeoX-20B: An Open-Source Autoregressive Language Model. In Angela Fan, Suzana Ilic, Thomas Wolf, and Matthias Gallé, editors, *Proceedings of BigScience Episode #5 – Workshop on Challenges & Perspectives in Creating Large Language Models*, pages 95–136, virtual+Dublin, 2022. Association for Computational Linguistics. doi: 10.18653/v1/2022.bigscience-1.9. URL <https://aclanthology.org/2022.bigscience-1.9/>.
- Kyunghyun Cho, Bart van Merriënboer, Caglar Gulcehre, Dzmitry Bahdanau, Fethi Bougares, Holger Schwenk, and Yoshua Bengio. Learning Phrase Representations using RNN Encoder-Decoder for Statistical Machine Translation. In *Proceedings of the 2014 Conference on Empirical Methods in Natural Language Processing*, pages 1724–1734, Doha, Qatar, 2014. Association for Computational Linguistics. doi: 10.3115/v1/D14-1179. URL <https://www.aclweb.org/anthology/D14-1179/>.
- Karl Cobbe, Vineet Kosaraju, Mohammad Bavarian, Mark Chen, Heewoo Jun, Lukasz Kaiser, Matthias Plappert, Jerry Tworek, Jacob Hilton, Reiichiro Nakano, Christopher Hesse, and John Schulman. Training Verifiers to

- Solve Math Word Problems, 2021. URL <http://arxiv.org/abs/2110.14168>. arXiv:2110.14168 [cs].
- Ben Cohen, Emaad Khwaja, Kan Wang, Charles Masson, Elise Ramé, Youssef Doubli, and Othmane Abou-Amal. Toto: Time Series Optimized Transformer for Observability, 2024. URL <http://arxiv.org/abs/2407.07874>. arXiv:2407.07874 [cs].
- Tri Dao and Albert Gu. Transformers are SSMS: Generalized Models and Efficient Algorithms Through Structured State Space Duality. In *Proceedings of the 41st International Conference on Machine Learning*, volume 235, pages 10041–10071, Vienna, Austria, 2024. PMLR. URL <https://proceedings.mlr.press/v235/dao24a.html>.
- Abhimanyu Das, Weihao Kong, Rajat Sen, and Yichen Zhou. A decoder-only foundation model for time-series forecasting. In *Proceedings of the 41st International Conference on Machine Learning*, volume 235, pages 10148–10167. PMLR, 2024. URL <https://proceedings.mlr.press/v235/das24c.html>.
- Gregoire Deletang, Anian Ruoss, Jordi Grau-Moya, Tim Genewein, Li Kevin Wenliang, Elliot Catt, Chris Cundy, Marcus Hutter, Shane Legg, Joel Veness, and Pedro A. Ortega. Neural Networks and the Chomsky Hierarchy. In *International Conference on Learning Representations*, volume 11. OpenReview, 2023. URL <https://openreview.net/forum?id=WbxHAzkeQcn>.
- Wei Du, Shubham Toshniwal, Branislav Kisacanin, Sadegh Mahdavi, Ivan Moshkov, George Armstrong, Stephen Ge, Edgar Minasyan, Feng Chen, and Igor Gitman. Nemotron-Math: Efficient Long-Context Distillation of Mathematical Reasoning from Multi-Mode Supervision, 2025. URL <https://arxiv.org/abs/2512.15489>. arXiv:2512.15489 [cs].
- Alexander M. Fichtl, Jeremias Bohn, Josefin Kelber, Edoardo Mosca, and Georg Groh. The End of Transformers? On Challenging Attention and the Rise of Sub-Quadratic Architectures, 2025. URL <http://arxiv.org/abs/2510.05364>. arXiv:2510.05364 [cs].
- Felix A. Gers, Jürgen Schmidhuber, and Fred Cummins. Learning to forget: continual prediction with LSTM. In *9th International Conference on Artificial Neural Networks ICANN '99*, pages 850–855, Edinburgh, UK, 1999. IET. ISBN 0 85296 721 7. doi: 10.1049/cp:19991218. URL <https://ieeexplore.ieee.org/document/818041>.
- Paolo Glorioso, Quentin Anthony, Yury Tokpanov, James Whittington, Jonathan Pilault, Adam Ibrahim, and Beren Millidge. Zamba: A Compact 7B SSM Hybrid Model, 2024. URL <http://arxiv.org/abs/2405.16712>. arXiv:2405.16712 [cs].
- Daniel Goldstein, Eric Alcaide, Janna Lu, and Eugene Cheah. RADLADS: Rapid Attention Distillation to Linear Attention Decoders at Scale. In *Conference on Language Modeling*, volume 2. OpenReview, 2025. URL <https://openreview.net/forum?id=38GehGepDd#discussion>. arXiv:2505.03005 [cs].
- Lars Graf, Thomas Ortner, Stanisław Woźniak, and Angeliki Pantazi. FlowState: Sampling-Rate Invariant Time Series Foundation Model with Dynamic Forecasting Horizons. In *Recent Advances in Time Series Foundation Models Have We Reached the 'BERT Moment'?* OpenReview, 2025. URL <https://openreview.net/forum?id=R50AT6nAsM>.
- Riccardo Grazi, Julien Siems, Arber Zela, Jörg K. H. Franke, Frank Hutter, and Massimiliano Pontil. Unlocking State-Tracking in Linear RNNs Through Negative Eigenvalues. In *International Conference on Learning Representations*, volume 13, Singapore, Singapore, 2025. URL <https://openreview.net/forum?id=UvTo3tVBk2>.
- Albert Gu and Tri Dao. Mamba: Linear-Time Sequence Modeling with Selective State Spaces. In *Conference on Language Modeling*, volume 1, Philadelphia, PA, USA, 2024. OpenReview. URL <https://openreview.net/forum?id=tEYskw1VY2>.
- Albert Gu, Karan Goel, and Christopher Re. Efficiently Modeling Long Sequences with Structured State Spaces. In *International Conference on Learning Representations*, volume 10. OpenReview, 2022. URL <https://openreview.net/forum?id=uYLFoz1v1AC>.
- Ankit Gupta, Albert Gu, and Jonathan Berant. Diagonal State Spaces are as Effective as Structured State Spaces. In *Advances in Neural Information Processing Systems*, volume 35, pages 22982–22994, New Orleans, LA, USA, 2022. Curran Associates, Inc. URL https://proceedings.neurips.cc/paper_files/paper/2022/hash/9156b0f6dfa9bbd18c79cc459ef5d61c-Abstract-Conference.html.
- Lukas Hauenberger, Niklas Schmidinger, Thomas Schmied, Anamaria-Roberta Hartl, David Stap, Pieter-Jan Hoedt, Maximilian Beck, Sebastian Böck, Günter Klambauer, and Sepp Hochreiter. Effective Distillation to Hybrid xLSTM Architectures, 2026. URL <https://arxiv.org/abs/2603.15590>. arXiv:2603.15590 [cs].
- Dan Hendrycks, Collin Burns, Saurav Kadavath, Akul Arora, Steven Basart, Eric Tang, Dawn Song, and Jacob Steinhardt. Measuring Mathematical Problem Solving With the MATH Dataset. In *Proceedings of the Neural Information Processing Systems Track on Datasets and Benchmarks*, volume 1. Curran Associates, Inc.,

2021. URL https://datasets-benchmarks-proceedings.neurips.cc/paper_files/paper/2021/hash/be83ab3ecd0db773eb2dc1b0a17836a1-Abstract-round2.html.
- Geoffrey Hinton, Oriol Vinyals, and Jeff Dean. Distilling the Knowledge in a Neural Network, 2015. URL <http://arxiv.org/abs/1503.02531>. arXiv:1503.02531 [stat].
- Sepp Hochreiter and Jürgen Schmidhuber. Long Short-Term Memory. *Neural Computation*, 9(8):1735–1780, 1997. ISSN 0899-7667, 1530-888X. doi: 10.1162/neco.1997.9.8.1735. URL <https://www.mitpressjournals.org/doi/abs/10.1162/neco.1997.9.8.1735>.
- Weizhe Hua, Zihang Dai, Hanxiao Liu, and Quoc Le. Transformer Quality in Linear Time. In *Proceedings of the 39th International Conference on Machine Learning*, volume 162, pages 9099–9117, Baltimore, MD, USA, 2022. PMLR. URL <https://proceedings.mlr.press/v162/hua22a.html>.
- Angelos Katharopoulos, Apoorv Vyas, Nikolaos Pappas, and François Fleuret. Transformers are RNNs: Fast Autoregressive Transformers with Linear Attention. In *Proceedings of the 37th International Conference on Machine Learning*, volume 119, pages 5156–5165, virtual, 2020. PMLR. URL <http://proceedings.mlr.press/v119/katharopoulos20a.html>.
- Disen Lan, Weigao Sun, Jiayi Hu, Jusen Du, and Yu Cheng. Liger: Linearizing Large Language Models to Gated Recurrent Structures. In *Proceedings of the 42nd International Conference on Machine Learning*, volume 267, pages 32452–32466. PMLR, 2025. URL <https://proceedings.mlr.press/v267/lan25b.html>.
- Hunter Lightman, Vineet Kosaraju, Yuri Burda, Harrison Edwards, Bowen Baker, Teddy Lee, Jan Leike, John Schulman, Ilya Sutskever, and Karl Cobbe. Let’s Verify Step by Step. In *International Conference on Learning Representations*, volume 12, Vienna, Austria, 2024. OpenReview. URL <https://openreview.net/forum?id=v8L0pN6EOi>.
- Bingbin Liu, Jordan Ash, Surbhi Goel, Akshay Krishnamurthy, and Cyril Zhang. Exposing Attention Glitches with Flip-Flop Language Modeling. In *Advances in Neural Information Processing Systems*, volume 36, pages 25549–25583. Curran Associates, Inc., 2023. URL https://proceedings.neurips.cc/paper_files/paper/2023/hash/510ad3018bbdc5b6e3b10646e2e35771-Abstract-Conference.html.
- Jean Mercat, Igor Vasiljevic, Sedrick Scott Keh, Kushal Arora, Achal Dave, Adrien Gaidon, and Thomas Kollar. Linearizing Large Language Models. In *Conference on Language Modeling*, volume 1. OpenReview, 2024. URL <https://openreview.net/forum?id=soGxskHGox>.
- William Merrill. Sequential Neural Networks as Automata. In Jason Eisner, Matthias Gallé, Jeffrey Heinz, Ariadna Quattoni, and Guillaume Rabusseau, editors, *Proceedings of the Workshop on Deep Learning and Formal Languages: Building Bridges*, pages 1–13, Florence, 2019. Association for Computational Linguistics. doi: 10.18653/v1/W19-3901. URL <https://aclanthology.org/W19-3901/>.
- William Merrill, Jackson Petty, and Ashish Sabharwal. The Illusion of State in State-Space Models. In *Proceedings of the 41st International Conference on Machine Learning*, volume 235, pages 35492–35506, Vienna, Austria, 2024. PMLR. URL <https://proceedings.mlr.press/v235/merrill124a.html>.
- William Merrill, Hongjian Jiang, Yanhong Li, Anthony Lin, and Ashish Sabharwal. Why Are Linear RNNs More Parallelizable?, 2026a. URL <http://arxiv.org/abs/2603.03612>. arXiv:2603.03612 [cs].
- William Merrill, Yanhong Li, Tyler Romero, Anej Svete, Caia Costello, Pradeep Dasigi, Dirk Groeneveld, David Heineman, Bailey Kuehl, Nathan Lambert, Chuan Li, Kyle Lo, Saumya Malik, D. J. Matusz, Benjamin Minixhofer, Jacob Morrison, Luca Soldaini, Finbarr Timbers, Pete Walsh, Noah A. Smith, Hannaneh Hajishirzi, and Ashish Sabharwal. Olmo Hybrid: From Theory to Practice and Back, 2026b. URL <http://arxiv.org/abs/2604.03444>. arXiv:2604.03444 [cs].
- Mayank Mishra. LM Engine: A Hyper-Optimized Library for Pretraining and Finetuning, 2024. URL <https://github.com/open-lm-engine/lm-engine>. original-date: 2024-09-03T19:45:30Z.
- Vladyslav Moroshan, Julien Siems, Arber Zela, Timur Carstensen, and Frank Hutter. TempoPFN: Towards Synthetic Pre-training of Linear RNNs for Zero-shot Time Series Forecasting. In *EurIPS Workshop: AI for Tabular Data*. OpenReview, 2025. URL <https://openreview.net/forum?id=Iqex1gfnvc#discussion>.
- NVIDIA. Nemotron 3 Nano: Open, Efficient Mixture-of-Experts Hybrid Mamba-Transformer Model for Agentic Reasoning, 2025. URL <http://arxiv.org/abs/2512.20848>. arXiv:2512.20848 [cs].
- Liliang Ren, Yang Liu, Yadong Lu, Yelong Shen, Chen Liang, and Weizhu Chen. Samba: Simple Hybrid State Space Models for Efficient Unlimited Context Language Modeling. In *International Conference on Learning Representations*, volume 13. OpenReview, 2025. URL <https://openreview.net/forum?id=bIlnpVM4bc>.
- Imanol Schlag, Kazuki Irie, and Jürgen Schmidhuber. Linear Transformers Are Secretly Fast Weight Programmers. In *Proceedings of the 38th International Conference on Machine Learning*, volume 139, pages 9355–9366, virtual, 2021. PMLR. URL <https://proceedings.mlr.press/v139/schlag21a.html>.

- Jürgen Schmidhuber. *Neural sequence chunkers*. Inst. für Informatik, 1991.
- Noam Shazeer. GLU Variants Improve Transformer, 2020. URL <http://arxiv.org/abs/2002.05202>. arXiv:2002.05202 [cs].
- Julien Siems, Timur Carstensen, Arber Zela, Frank Hutter, Massimiliano Pontil, and Riccardo Grazi. DeltaProduct: Improving State-Tracking in Linear RNNs via Householder Products. In *Advances in Neural Information Processing Systems*, volume 38, pages 153738–153782. Curran Associates, Inc., 2025. URL https://proceedings.neurips.cc/paper_files/paper/2025/hash/e1ea2520fbf9cd1600b287dde67e0a3c-Abstract-Conference.html.
- Julien Siems, Riccardo Grazi, Kirill Kalinin, Hitesh Ballani, and Babak Rahmani. Learning State-Tracking from Code Using Linear RNNs, 2026. URL <https://arxiv.org/abs/2602.14814>. arXiv:2602.14814 [cs].
- Jamba Team. Jamba: Hybrid Transformer-Mamba Language Models. In *International Conference on Learning Representations*, volume 13. OpenReview, 2025a. URL <https://openreview.net/forum?id=JFPaD71pBD>. arXiv:2403.19887 [cs].
- Kimi Team. Kimi Linear: An Expressive, Efficient Attention Architecture, 2025b. URL <http://arxiv.org/abs/2510.26692>. arXiv:2510.26692 [cs].
- Qwen Team. Qwen3 Technical Report, 2025c. URL <http://arxiv.org/abs/2505.09388>. arXiv:2505.09388 [cs].
- Ashish Vaswani, Noam Shazeer, Niki Parmar, Jakob Uszkoreit, Llion Jones, Aidan N. Gomez, Lukasz Kaiser, and Illia Polosukhin. Attention Is All You Need. In *Advances in Neural Information Processing Systems*, volume 30, pages 5998–6008, Long Beach, CA, USA, 2017. Curran Associates, Inc. URL <https://proceedings.neurips.cc/paper/2017/hash/3f5ee243547dee91fbd053c1c4a845aa-Abstract.html>.
- Junxiong Wang, Daniele Paliotta, Avner May, Alexander M. Rush, and Tri Dao. The Mamba in the Llama: Distilling and Accelerating Hybrid Models. In *Advances in Neural Information Processing Systems*, volume 37, pages 62432–62457, Vancouver, BC, Canada, 2024. Curran Associates, Inc. doi: 10.52202/079017-1996. URL https://proceedings.neurips.cc/paper_files/paper/2024/hash/723933067ad315269b620bc0d2c05cba-Abstract-Conference.html.
- Gail Weiss, Yoav Goldberg, and Eran Yahav. On the Practical Computational Power of Finite Precision RNNs for Language Recognition. In Iryna Gurevych and Yusuke Miyao, editors, *Proceedings of the 56th Annual Meeting of the Association for Computational Linguistics*, volume 2, pages 740–745, Melbourne, Australia, 2018. Association for Computational Linguistics. doi: 10.18653/v1/P18-2117. URL <https://aclanthology.org/P18-2117/>.
- Gerald Woo, Chenghao Liu, Akshat Kumar, Caiming Xiong, Silvio Savarese, and Doyen Sahoo. Unified Training of Universal Time Series Forecasting Transformers. In *Proceedings of the 41st International Conference on Machine Learning*, volume 235, pages 53140–53164. PMLR, 2024. URL <https://proceedings.mlr.press/v235/woo24a.html>.
- Yuxin Wu and Kaiming He. Group Normalization. In Vittorio Ferrari, Martial Hebert, Cristian Sminchisescu, and Yair Weiss, editors, *Computer Vision – ECCV 2018*, pages 3–19, Munich, Germany, 2018. Springer International Publishing. ISBN 978-3-030-01261-8. doi: 10.1007/978-3-030-01261-8_1. URL https://openaccess.thecvf.com/content_ECCV_2018/html/Yuxin_Wu_Group_Normalization_ECCV_2018_paper.html.
- Guangxuan Xiao, Yuandong Tian, Beidi Chen, Song Han, and Mike Lewis. Efficient Streaming Language Models with Attention Sinks. In *International Conference on Learning Representations*, volume 12, Vienna, Austria, 2024. OpenReview. URL <https://openreview.net/forum?id=NG7sS51zVF>.
- Songlin Yang and Yu Zhang. FLA: A Triton-Based Library for Hardware-Efficient Implementations of Linear Attention Mechanism, 2026. URL <https://github.com/fla-org/flash-linear-attention>. original-date: 2023-12-20T06:50:18Z.
- Songlin Yang, Bailin Wang, Yikang Shen, Rameswar Panda, and Yoon Kim. Gated Linear Attention Transformers with Hardware-Efficient Training. In *Proceedings of the 41st International Conference on Machine Learning*, volume 235, pages 56501–56523, Vienna, Austria, 2024a. PMLR. URL <https://proceedings.mlr.press/v235/yang24ab.html>.
- Songlin Yang, Bailin Wang, Yu Zhang, Yikang Shen, and Yoon Kim. Parallelizing Linear Transformers with the Delta Rule over Sequence Length. In *Advances in Neural Information Processing Systems*, volume 37, pages 115491–115522, Vancouver, BC, Canada, 2024b. Curran Associates, Inc. doi: 10.52202/079017-3668. URL https://proceedings.neurips.cc/paper_files/paper/2024/hash/d13a3eae72366e61dfdc7eea82eeb685-Abstract-Conference.html.
- Michael Zhang, Simran Arora, Rahul Chalamala, Benjamin Frederick Spector, Alan Wu, Krithik Ramesh,

Aaryan Singhal, and Christopher Re. LoLCATs: On Low-Rank Linearizing of Large Language Models. In *International Conference on Learning Representations*, volume 13, Singapore, Singapore, 2025. OpenReview. URL <https://openreview.net/forum?id=8VtGeyJyx9>.

Appendix

A	Notation table	17
B	Code-focused Language Model Pre-training Results	19
C	Distillation Results	20
	C.1 Distillation: Full Pass@ k on HumanEval	20
	C.2 Distillation Results on Math Data	20
D	Time-series Foundation-Model Pre-training Results	21
E	Synthetic Task Results	22
F	Experimental & Implementation Details	22
	F.1 Language Model Pretraining	22
	F.2 Linearization via Distillation	22
	F.3 Pretraining Time Series Foundation Models	24
	F.4 Synthetic Counting and State-tracking Experiments	25
G	Related Linearization Work	25

A Notation table

Table 2: Notation used in this paper.

Symbol	Definition	Type
<i>General sequence notation</i>		
t	Time step index	scalar
T	Total sequence length	scalar
n	Chunk index, $1 \leq n \leq \lceil T/C \rceil$	scalar
C	Chunk size	scalar
D	Input / model dimensionality	scalar
D_{qk}	Query and key dimensionality	scalar
D_v	Value dimensionality	scalar
\mathbf{x}_t	Input vector at time step t	\mathbb{R}^D
\mathbf{X}	Input sequence matrix	$\mathbb{R}^{T \times D}$
\mathbf{H}	Output sequence matrix	$\mathbb{R}^{T \times D_v}$
<i>Attention mechanism</i>		
\mathbf{q}_t	Query vector at time step t	$\mathbb{R}^{D_{\text{qk}}}$
\mathbf{k}_t	Key vector at time step t	$\mathbb{R}^{D_{\text{qk}}}$
\mathbf{v}_t	Value vector at time step t	\mathbb{R}^{D_v}
\mathbf{Q}	Stacked query matrix	$\mathbb{R}^{T \times D_{\text{qk}}}$
\mathbf{K}	Stacked key matrix	$\mathbb{R}^{T \times D_{\text{qk}}}$
\mathbf{V}	Stacked value matrix	$\mathbb{R}^{T \times D_v}$
\mathbf{W}_q	Query projection weight matrix	$\mathbb{R}^{D_{\text{qk}} \times D}$
\mathbf{W}_k	Key projection weight matrix	$\mathbb{R}^{D_{\text{qk}} \times D}$
\mathbf{W}_v	Value projection weight matrix	$\mathbb{R}^{D_v \times D}$
\mathbf{M}	Causal masking matrix, $m_{ij} = 1$ iff $i \geq j$	$\{0, 1\}^{T \times T}$
\mathbf{C}_t	Matrix cell state / linear-attention memory at time t	$\mathbb{R}^{D_{\text{qk}} \times D_v}$
\mathbf{n}_t	Normalizer state at time step t	$\mathbb{R}^{D_{\text{qk}}}$
<i>xLSTM[0:1] – nonlinear recurrent component (sLSTM)</i>		
\mathbf{h}_t	Hidden state at time step t	\mathbb{R}^D
\mathbf{c}_t	Cell state at time step t	\mathbb{R}^D
\mathbf{i}_t	Input gate vector at time step t (exponential activation)	\mathbb{R}^D
\mathbf{f}_t	Forget gate vector at time step t (σ activation)	\mathbb{R}^D
$\mathbf{W}_i, \mathbf{W}_f, \mathbf{W}_v$	Input weight matrices for input gate, forget gate, cell input	$\mathbb{R}^{D \times D}$
$\mathbf{R}_i, \mathbf{R}_f, \mathbf{R}_v$	Recurrent weight matrices for input gate, forget gate, cell input	$\mathbb{R}^{D \times D}$
<i>xLSTM[1:0] – linear attention component (mLSTM)</i>		
i_t	Scalar input gate at time step t (exponential activation)	scalar $\in \mathbb{R}$
f_t	Scalar forget gate at time step t (σ activation)	scalar $\in \mathbb{R}$
\mathbf{w}_i	Weight vector for input gate	\mathbb{R}^D
\mathbf{w}_f	Weight vector for forget gate	\mathbb{R}^D
<i>xLSTM[m:s] – full architecture</i>		
m	Number of linear-attention layers (xLSTM[1:0] blocks)	scalar

Table 2 – continued

Symbol	Definition	Type
s	Number of nonlinear recurrent layers (xLSTM[0:1] blocks)	scalar
<i>Mamba-2</i>		
\mathbf{w}_Δ	Weight vector for sample-time (discretization) projection	\mathbb{R}^D
a	Non-negative learned parameter for 1-SS transition matrix	scalar $\in \mathbb{R}_{\geq 0}$
<i>Gated DeltaNet</i>		
\mathbf{w}_α	Weight vector for forget gate	\mathbb{R}^D , scalar
\mathbf{w}_β	Weight vector for write-strength gate	\mathbb{R}^D , scalar
<i>Activation functions and operators</i>		
\tanh	Hyperbolic tangent; cell input activation in xLSTM[0:1]	function
σ	Sigmoid function; forget and output gate activation	function
\exp	Exponential function; input gate in xLSTM	function
softplus	Softplus function; input gate in Mamba-2	function
softmax	Softmax function; attention normalization	function
\odot	Element-wise (Hadamard) product	operator
\otimes	Outer product	operator
$\ \mathbf{v}\ $	Euclidean norm of vector $\mathbf{v} \in \mathbb{R}^D$	scalar
$\text{diag}(\mathbf{v})$	Diagonal matrix with entries $\mathbf{v} \in \mathbb{R}^D$	$\mathbb{R}^{D \times D}$
<i>Architecture mappings</i>		
$\text{xLSTM}[m:s](\cdot)$	Hybrid xLSTM with m mLSTM and s sLSTM layers	$\mathbb{R}^{T \times D} \rightarrow \mathbb{R}^{T \times D}$
$\text{Mamba-2}(\cdot)$	Mamba-2 layer mapping	$\mathbb{R}^{T \times D} \rightarrow \mathbb{R}^{T \times D}$
$\text{GatedDeltaNet}(\cdot)$	Gated DeltaNet layer mapping	$\mathbb{R}^{T \times D} \rightarrow \mathbb{R}^{T \times D}$
<i>Evaluation metrics</i>		
MASE	Mean Absolute Scaled Error (time-series evaluation)	scalar
CRPS	Continuous Ranked Probability Score (time-series evaluation)	scalar
$\text{pass}@k$	Code generation pass rate over $k \in \mathbb{N}$ samples	scalar

B Code-focused Language Model Pre-training Results

This appendix reports the full numerical results for the code-focused language-model pre-training experiments in Section 2.1. The main text focuses on the cross-family comparison between Gated DeltaNet, Mamba-2, and xLSTM [7:1]. Here, we additionally report xLSTM [1:0] and xLSTM [11:1] to show how the linear-attention-to-recurrent-layer ratio affects performance within the xLSTM family. All models are 400M-parameter inter-layer hybrids trained with the same recipe; only the sequence-operator configuration changes.

Code generation. Tables 3, 4, and 5 report the full HumanEval pass@ k results. Across all three training configurations, xLSTM [7:1] is the best model at every reported pass@ k . The strongest non-xLSTM baseline changes with data and scale: Gated DeltaNet is second-best on both 20B-token and 100B code-only settings, while Mamba-2 is second-best on the mixed Nemotron-CC-Code-v1 + FineWeb-Edu corpus. The additional xLSTM variants show that the xLSTM layer ratio matters: xLSTM [1:0] and xLSTM [11:1] are competitive in some cells, but neither matches the consistent HumanEval performance of xLSTM [7:1].

Enabling negative eigenvalues in the state-transition matrix (Grazzi et al., 2025) Gated DeltaNet [-1:1] does not bring a substantial improvement for hybrid language model pretraining on code, as also observed by Merrill et al. (2026b). However, in other tasks presented in Section F.3 and Sections F.4, we observe that the specific state tracking capabilities enabled by the negative eigenvalues yield clear improvements.

Table 3: HumanEval pass@ k ($k \in \{2, 8, 16, 64\}$, %) for 400M-parameter inter-layer hybrid variants pretrained on Nemotron-CC-Code-v1 for 20B tokens. Higher is better; the best result per column is shown in **bold**.

Model	pass@2 \uparrow	pass@8 \uparrow	pass@16 \uparrow	pass@64 \uparrow
xLSTM [1:0]	1.42	3.67	5.34	8.53
xLSTM [7:1]	2.71	5.92	7.80	12.13
xLSTM [11:1]	2.60	5.16	6.82	10.20
Mamba-2	1.90	3.93	5.25	8.68
Gated DeltaNet	2.29	4.62	6.17	10.70
Gated DeltaNet [-1, 1]	2.09	4.28	5.68	9.41

Table 4: HumanEval pass@ k ($k \in \{2, 8, 16, 64\}$, %) for 400M-parameter inter-layer hybrid variants pretrained on Nemotron-CC-Code-v1 for 100B tokens. Higher is better; the best result per column is shown in **bold**.

Model	pass@2 \uparrow	pass@8 \uparrow	pass@16 \uparrow	pass@64 \uparrow
xLSTM [1:0]	3.21	6.66	8.54	13.09
xLSTM [7:1]	4.61	9.33	11.56	15.84
xLSTM [11:1]	4.04	7.42	9.41	13.14
Mamba-2	4.00	7.73	9.97	14.36
Gated DeltaNet	3.75	7.76	10.05	14.94
Gated DeltaNet [-1, 1]	3.33	6.02	7.92	13.07

Reasoning and commonsense. Tables 6, 7, and 8 report the full reasoning and commonsense results. Among the three cross-family backbones discussed in the main text, xLSTM [7:1] has the best aggregate score in all three training configurations. The margins are small compared with the HumanEval results, which supports the main-text conclusion that broad reasoning and commonsense evaluations are less sensitive to these backbone differences than code generation is. The additional xLSTM-ratio ablations show a more mixed pattern: xLSTM [11:1] gives the best aggregate score in

Table 5: HumanEval pass@ k ($k \in \{2, 8, 16, 64\}$, %) for 400M-parameter inter-layer hybrid variants pretrained on Nemotron-CC-Code-v1 + FineWeb-Edu for 20B tokens. Higher is better; the best result per column is shown in **bold**.

Model	pass@2 \uparrow	pass@8 \uparrow	pass@16 \uparrow	pass@64 \uparrow
xLSTM [1:0]	0.88	1.96	3.01	6.40
xLSTM [7:1]	2.26	4.68	6.00	9.50
xLSTM [11:1]	1.81	3.29	4.20	7.17
Mamba-2	2.07	3.81	4.79	7.69
Gated DeltaNet	1.54	2.97	3.98	7.36
Gated DeltaNet [-1, 1]	1.26	3.00	4.20	7.25

the 20B-token mixed corpus setting, while xLSTM [7:1] gives the best aggregate score at pure code on both 20B and 100B tokens.

Table 6: Reasoning and commonsense benchmark results for 400M-parameter inter-layer hybrid variants pretrained on Nemotron-CC-Code-v1 for 20B tokens. Higher is better; the best result per column is shown in **bold**.

Training data	Model	Reasoning / Commonsense (%)					
		HellaSwag \uparrow	PIQA \uparrow	ARC-Easy \uparrow	ARC-Challenge \uparrow	WinoGrande \uparrow	Avg. \uparrow
Nemotron-CC-Code-v1 (20B tokens)	xLSTM [1:0]	28.29	56.80	32.07	22.18	52.57	38.38
	xLSTM [7:1]	29.50	58.38	33.88	21.16	50.91	38.76
	xLSTM [11:1]	29.67	57.40	34.05	22.01	49.64	38.55
	Mamba-2	29.37	57.56	34.30	21.42	50.75	38.68
	Gated DeltaNet	29.43	56.86	33.42	22.70	50.91	38.66
	Gated DeltaNet [-1, 1]	29.29	56.69	33.08	23.38	49.80	38.45

Table 7: Reasoning and commonsense benchmark results for 400M-parameter inter-layer hybrid variants pretrained on Nemotron-CC-Code-v1 for 100B tokens. Higher is better; the best result per column is shown in **bold**.

Training data	Model	Reasoning / Commonsense (%)					
		HellaSwag \uparrow	PIQA \uparrow	ARC-Easy \uparrow	ARC-Challenge \uparrow	WinoGrande \uparrow	Avg. \uparrow
Nemotron-CC-Code-v1 (100B tokens)	xLSTM [1:0]	30.13	58.38	34.68	23.29	49.49	39.19
	xLSTM [7:1]	31.38	57.56	36.32	22.18	52.09	39.91
	xLSTM [11:1]	30.11	57.94	35.23	21.76	52.17	39.44
	Mamba-2	30.06	58.98	35.48	21.67	50.91	39.42
	Gated DeltaNet	30.23	56.75	35.61	22.01	51.38	39.20
	Gated DeltaNet [-1, 1]	29.64	58.76	34.68	21.59	48.93	38.72

C Distillation Results

C.1 Distillation: Full Pass@ k on HumanEval

Table 9 reports the full pass@ k spread for $k \in \{1, 2, 8, 16, 32, 64\}$ on HumanEval and HumanEval+ for the code distilled students discussed in Section 2.2. All students follow the recipe described in Appendix F.2. The xLSTM [1:0] student remains strongest at every k on both benchmarks. Gated DeltaNet [-1, 1] improves over default Gated DeltaNet at every k on HumanEval and HumanEval+, but does not close the gap to xLSTM [1:0].

C.2 Distillation Results on Math Data

Table 10 reports the math-distillation results for the same two student operators. The xLSTM [1:0] student leads on GSM8K and AIME 2024 pass@8, while Gated DeltaNet is slightly stronger on

Table 8: Reasoning and commonsense benchmark results for 400M-parameter inter-layer hybrid variants pretrained on Nemotron-CC-Code-v1 + FineWeb-Edu for 20B tokens. Higher is better; the best result per column is shown in **bold**.

Training data	Model	Reasoning / Commonsense (%)					
		HellaSwag \uparrow	PIQA \uparrow	ARC-Easy \uparrow	ARC-Challenge \uparrow	WinoGrande \uparrow	Avg. \uparrow
Nemotron-CC-Code-v1 + FineWeb-Edu (20B tokens)	xLSTM [1:0]	33.11	62.62	47.18	25.09	51.22	43.84
	xLSTM [7:1]	35.81	64.80	47.73	25.91	49.72	44.79
	xLSTM [11:1]	35.36	64.25	46.97	26.88	52.64	45.22
	Mamba-2	34.98	64.15	46.97	25.60	49.64	44.27
	Gated DeltaNet	34.94	64.09	47.26	26.19	50.83	44.66
	Gated DeltaNet [-1,1]	35.00	63.71	46.00	26.19	51.62	44.50

Table 9: Full pass@ k spread on HumanEval and HumanEval+ for the code distilled students. Higher is better; the best student result per column is shown in **bold**.

Benchmark	Student	$k = 1 \uparrow$	$k = 2 \uparrow$	$k = 8 \uparrow$	$k = 16 \uparrow$	$k = 32 \uparrow$	$k = 64 \uparrow$
HumanEval	Qwen3-4B-Instruct (teacher)	0.914	0.927	0.944	0.950	0.956	0.963
	xLSTM [1:0]	0.831	0.882	0.940	0.952	0.956	0.957
	Gated DeltaNet	0.802	0.845	0.892	0.905	0.914	0.921
	Gated DeltaNet [-1,1]	0.813	0.854	0.897	0.912	0.922	0.927
HumanEval+	Qwen3-4B-Instruct (teacher)	0.835	0.848	0.859	0.862	0.864	0.866
	xLSTM [1:0]	0.764	0.808	0.863	0.878	0.889	0.896
	Gated DeltaNet	0.739	0.780	0.832	0.846	0.856	0.866
	Gated DeltaNet [-1,1]	0.745	0.784	0.840	0.862	0.877	0.884

MATH-500. Averaged across GSM8K, MATH-500, and AIME pass@8, xLSTM [1:0] reaches 0.645 compared with 0.625 for Gated DeltaNet. Table 11 reports the full AIME 2024 pass@ k breakdown.

Table 10: Math distillation results for students distilled from Qwen3-4B-Instruct with the matched recipe of HAUZENBERGER et al. (2026). GSM8K and MATH-500 report exact match (COBBE et al., 2021; HENDRYCKS et al., 2021; LIGHTMAN et al., 2024); AIME 2024 reports pass@8. The Avg. column averages GSM8K, MATH-500, and AIME pass@8. Higher is better; the best student result per column is shown in **bold**.

Student	GSM8K \uparrow	MATH-500 \uparrow	AIME pass@8 \uparrow	Avg. \uparrow
Qwen3-4B-Instruct (teacher)	0.939	0.854	0.367	0.720
xLSTM [1:0]	0.876	0.726	0.333	0.645
Gated DeltaNet	0.842	0.732	0.300	0.625

D Time-series Foundation-Model Pre-training Results

This appendix reports the full numerical results for the time-series foundation-model pre-training experiments in Section 2.3. All models use the same time-series pre-training protocol of AUER et al. (2025); only the sequence mixer changes. We evaluate zero-shot on GIFT-Eval (AKSU et al., 2024) and report MASE and CRPS, aggregated by geometric mean. Lower values are better.

Table 12 shows the scaling comparison across five parameter scales. We additionally also train Gated DeltaNet with the negative eigenvalues enabled in the state transition matrix, as described in GRAZZI et al. (2025) and report the results in the table. xLSTM [3:1] gives the best result on both metrics from 1M to 40M parameters. At 80M parameters, the architectures nearly converge: xLSTM,[3:1] and Mamba-2 match on MASE, while Mamba-2 is best on CRPS. Notably, Gated DeltaNet with negative eigenvalues performs better than its non-negative counterpart, implying that time series foundation models benefit from the specific state tracking capacity enabled by this modification.

Table 11: Full pass@ k breakdown on AIME 2024 for the two distilled students. Higher is better; the best student result per column is shown in **bold**.

Student	$k = 1 \uparrow$	$k = 2 \uparrow$	$k = 4 \uparrow$	$k = 8 \uparrow$	$k = 16 \uparrow$	$k = 32 \uparrow$
Qwen3-4B-Instruct (teacher)	0.250	0.302	0.344	0.367	0.367	0.367
xLSTM [1:0]	0.055	0.105	0.190	0.333	0.333	0.333
Gated DeltaNet	0.052	0.101	0.183	0.300	0.300	0.300

Table 12: GIFT-Eval scores for time-series foundation models. Models are evaluated zero-shot on GIFT-Eval, and results are aggregated by geometric mean. Lower is better; the best result per scale and metric is shown in **bold**.

Model	1M		4M		10M		40M		80M	
	MASE \downarrow	CRPS \downarrow	MASE \downarrow	CRPS \downarrow	MASE \downarrow	CRPS \downarrow	MASE \downarrow	CRPS \downarrow	MASE \downarrow	CRPS \downarrow
xLSTM [3:1]	0.768	0.527	0.739	0.509	0.733	0.508	0.716	0.493	0.715	0.490
Mamba-2	0.795	0.545	0.784	0.533	0.767	0.525	0.721	0.496	0.715	0.485
Gated DeltaNet	0.882	0.609	0.826	0.566	0.817	0.561	0.792	0.550	0.735	0.502
Gated DeltaNet [-1, 1]	0.792	0.541	0.766	0.521	0.764	0.517	0.720	0.496	0.714	0.489

E Synthetic Task Results

Table 13 presents the results for all synthetic tasks across the three evaluated sequence lengths: 128 (training length), 512 and 2048.

Table 13: Length generalization of sequence mixers on synthetic counting and state-tracking tasks. Models are trained at a sequence length of 128 and evaluated at 128, 512, and 2048. Report accuracy (%).

Model	Counting									State Tracking								
	$A^n B^n$			$A^n B^n C^n$			Majority			Parity			Mod. Arith.			S_3		
	128	512	2048	128	512	2048	128	512	2048	128	512	2048	128	512	2048	128	512	2048
xLSTM[1:0]	1.000	0.963	0.892	1.000	0.984	0.932	1.000	0.982	0.763	0.013	0.001	0.003	0.314	0.292	0.283	0.088	0.022	0.003
xLSTM[1:1]	1.000	0.943	0.834	1.000	0.997	0.716	1.000	0.975	0.742	1.000	1.000	1.000	1.000	1.000	1.000	1.000	1.000	1.000
Mamba-2	1.000	0.852	0.241	0.839	0.808	0.443	0.998	0.800	0.366	0.352	0.087	0.012	0.425	0.391	0.383	0.272	0.074	0.009
Gated DeltaNet	1.000	0.993	0.820	0.981	0.805	0.322	0.991	0.717	0.268	0.060	0.014	0.003	0.361	0.340	0.328	0.141	0.036	0.004
Gated DeltaNet[-1,1]	1.000	0.993	0.983	1.000	0.582	0.233	1.000	0.776	0.317	1.000	1.000	0.472	0.495	0.468	0.452	1.000	1.000	0.667

F Experimental & Implementation Details

F.1 Language Model Pretraining

Pretraining Data. We utilized the Nemotron-CC-Code-v1 and FineWeb Edu (100B subset) datasets, tokenized with GPT-NeoX tokenizer (Black et al., 2022).

Model Hyperparameters. Table 14 reports hyperparameters of the pretrained language models and Table 15 provides the evaluation details. For Gated DeltaNet, Mamba 2 and Attention we took the defaults settings from the `lm-engine` (Mishra, 2024) library and for xLSTM we took the setup of Beck et al. (2026) to achieve a matched 400m parameter count for all models. All models are pre-norm architectures with RMSNorm.

Training Setup. All models were trained on 8xH100 GPUs using bfloat16 and PyTorch Distributed Data Parallel (DDP).

F.2 Linearization via Distillation

This appendix expands the distillation recipe of HAUZENBERGER et al. (2026) used in Section 2.2. The recipe replaces every softmax-attention block of a Transformer teacher with an intra-layer hybrid

Table 14: Hyperparameters for Language Model Pretraining at 400M scale.

Setting	Value
Hidden Size	1024
Num Layers	24
Positional Encoding	NoPE
Num Heads (xLSTM/GDN)	4
Num Heads (Attention)	16
Num Heads (Mamba)	64
Conv Kernel Size	4
Context size	8192
Optimizer	AdamW
LR Scheduler	Cosine + Warmup
Warmup %	10%
Weight decay	0.1
Learning rate	3e-4
Gradient Clipping	1.0
Effective Batch Size	128
Tokens per Step	1M
Attention Layer idx	[6, 14, 22]
MLP Expansion Factor	2.75
Activation Function	SwiGLU

Table 15: Evaluation setup details for language model pre-training.

Task	# of shots	Generation Budget
<i>Language Understanding</i>		
PIQA	0	–
ARC-e	0	–
ARC-c	25	100
HellaSwag	10	–
Winogrande	5	–
<i>Language Generation</i>		
HumanEval	0	1024

block that combines a linear-attention replacement with a sliding-window-attention path. In our experiments, the linear-attention replacement is xLSTM [1:0], default Gated DeltaNet, or, for code distillation, Gated DeltaNet [−1, 1]. The replacement inherits the teacher’s \mathbf{q} , \mathbf{k} , and \mathbf{v} projection weights at initialization. Training proceeds in two stages: hidden-state alignment followed by sparse knowledge distillation. We omit the optional expert-merging step of HAUZENBERGER ET AL. (2026).

Recipe compatibility. The recipe supports a candidate operator as a plug-in replacement when it exposes query, key, and value projections, admits a matrix-state formulation compatible with chunkwise-parallel kernels, and accepts the feature maps used by the scaffold. xLSTM [1:0], Gated DeltaNet, and Gated DeltaNet [−1, 1] satisfy these requirements. xLSTM [0:1] does not, because it is sequential and has no query-key-value analogue to initialize from the teacher. Mamba-2 also requires a recipe extension: its input and forget gates are tied through a learned projection and scalar transition parameter, which do not have a direct teacher-attention analogue. For this reason, Section 2.2 isolates xLSTM [1:0] and Gated DeltaNet variants as plug-in matrix-state operators.

Hybrid block. Each multi-head-attention block of the teacher is replaced by an intra-layer hybrid block whose output for token t is

$$\hat{\mathbf{h}}_t = \mathbf{o}_t \odot \text{LinAtt}(\mathbf{q}_t, \mathbf{k}_t, \mathbf{v}_t) + (\mathbf{1} - \mathbf{o}_t) \odot \text{SWA}(\mathbf{q}_t, \mathbf{k}_t, \mathbf{v}_t), \quad (5)$$

where LinAtt is the linear-attention operator, SWA is sliding-window attention with window size 512 and four prepended sink tokens (Xiao et al., 2024; Beltagy et al., 2020), and $\mathbf{o}_t \in (0, 1)^H$ is a per-head data-dependent sigmoid gate computed from the concatenation $[\mathbf{q}_t, \mathbf{k}_t, \mathbf{v}_t]$. We apply rotary positional embeddings to \mathbf{q}_t and \mathbf{k}_t . The xLSTM [1:0] branch uses head-wise softmax feature maps over the feature dimension and per-head scalar output gates; we keep the original xLSTM [1:0] normalizer.

Stage I: hidden-state alignment. With teacher and student forward passes evaluated on the same input, we minimize the per-layer mean-squared error between teacher attention outputs $\mathbf{h}_t^{(\ell)}$ and student hybrid-block outputs $\hat{\mathbf{h}}_t^{(\ell)}$:

$$\mathcal{L}_{\text{align}} = \sum_{\ell} \sum_t \|\mathbf{h}_t^{(\ell)} - \hat{\mathbf{h}}_t^{(\ell)}\|_2^2. \quad (6)$$

Only the newly introduced parameters, including feature maps and gates, are trainable in this stage. Embeddings and feed-forward blocks remain frozen.

Stage II: sparse knowledge distillation. With all parameters unfrozen, we minimize a convex combination of next-token cross-entropy and a sparse top- k KL divergence between the teacher and student output distributions:

$$\mathcal{L}_{\text{KD}} = -\gamma \sum_t \log p_{\theta}(y_t | \mathbf{x}_{1:t}) + \beta \sum_t \text{KL}[p_T^{(k)}(\cdot | \mathbf{x}_{1:t}) \| p_{\theta}^{(k)}(\cdot | \mathbf{x}_{1:t})], \quad (7)$$

where $p_T^{(k)}$ and $p_{\theta}^{(k)}$ are the top- k truncations of the teacher and student distributions. We set $\gamma = 0.9$, $\beta = 0.1$, and $k = 256$. Sparsifying the teacher distribution allows precomputing teacher targets, so the teacher does not need to run during Stage II.

Hyperparameters. Sequence length is 4,096 throughout. Stage II trains for 10,000 optimization steps in each domain. Code distillation uses Nemotron-Pretraining-Code-v2 (NVIDIA, 2025). Math distillation uses Nemotron-Math-v2 (Du et al., 2025). Optimizer, learning-rate schedule, and remaining hyperparameters follow Hauzenberger et al. (2026) unchanged.

Gated DeltaNet variants. The Gated DeltaNet branch follows the recipe defaults: rotary-positioned queries and keys, SiLU feature maps applied to \mathbf{q} , \mathbf{k} , and \mathbf{v} , qk L^2 -normalization inside the kernel, recurrent-gate clamping at -3 , document-boundary resets with reset value -25 , and an unmerged background gating head. The recurrent branch uses the chunk kernel during training and inference. For code distillation, Gated DeltaNet $[-1, 1]$ keeps the same scaffold, data, initialization, and optimization recipe, but uses the negative-eigenvalue parameterization of Grazi et al. (2025). We do not enable this variant in the math-distillation runs, because the corresponding xLSTM $[m:s]$ extension is outside the scope of the matched plug-in comparison.

F.3 Pretraining Time Series Foundation Models

Pretraining Data. The time series foundation models were pretrained on a corpus of $\sim 47.5\text{M}$ timeseries, based on Auer et al. (2025). This consists of $\sim 30\text{M}$ series from the Chronos pretraining corpus introduced in Ansari et al. (2024), $\sim 2.5\text{M}$ series from the GIFT-Eval Pretraining corpus introduced in Aksu et al. (2024), and $\sim 15\text{M}$ series synthetically generated using KernelSynth (Ansari et al., 2024). The data corpus has been cleaned for zero overlap with the GIFT-Eval training corpus, hence all evaluations are zero-shot.

Training Setup. All time series models were trained on 4x NVIDIA A100 GPUs using bfloat16 and PyTorch Distributed Data Parallel (DDP). All model hyperparameters are reported in Tables 17 and 16

Table 16: **Architecture hyperparameters for the five parameter scales used throughout TSFM experiments.** Width (hidden dimension), depth (number of layers), input/output projection (“linear” at 1M, residual-MLP with the listed hidden dimension otherwise), MLP expansion factor and number of heads. All backbones at a given scale share these settings.

Scale	Width	Depth	In/Out proj.	MLP exp.	Num Heads
1M	128	6	linear	2.0	4
4M	256	6	MLP, 1024	2.0	4
10M	384	6	MLP, 2048	2.0	3
40M	512	12	MLP, 2048	2.75	4
80M	768	12	MLP, 2048	2.75	6

F.4 Synthetic Counting and State-tracking Experiments

Tasks. We evaluate sequence mixers on six synthetic formal-language tasks split into two families. The counting family contains $A^n B^n$ (balanced two-symbol strings), $A^n B^n C^n$ (balanced three-symbol strings), and Majority (predict the majority symbol over an input sequence). The state-tracking family contains Parity (predict the running XOR of a binary sequence), Modular Arithmetic over \mathbb{Z}_5 (running sum modulo 5), and word-problem evaluation in the symmetric group S_3 (composition of permutations on three elements).

Data. For each task, training samples are drawn at a sequence length of 128. Evaluation samples are drawn at three lengths: 128 (in-distribution), 512 ($4\times$ extrapolation), and 2048 ($16\times$ extrapolation). At each evaluation length, we sample a held-out test set disjoint from training. The model is required to output the task target at the final position of the sequence.

Training Setup. All models are trained from scratch at a sequence length of 128. Models are trained on a single NVIDIA H100 GPU using bfloat16. We used two block structures without MLP layers. We report all training hyperparameters in Table 18.

Evaluation. We report token-level accuracy at the target position, averaged over the held-out evaluation set at each length. We run each experiment over 5 seeds and report the maximum of those runs.

G Related Linearization Work

Existing linearization work converts Transformer language models into subquadratic students, but typically fixes the target operator family. LoLCATs (Zhang et al., 2025) replaces softmax attention with an intra-layer hybrid of linear and sliding-window attention, fitting the linearization at the layer level rather than comparing candidate sequence mixers. Liger (Lan et al., 2025) linearizes language models into gated recurrent structures through gating-only modifications. RADLADS (Goldstein et al., 2025) distills RWKV-6/7 backbones with an RWKV-specific pipeline. Llamba (Bick et al., 2025) converts attention layers to Mamba-2 state-space mixers, and MOHAWK (Bick et al., 2024) aligns Transformer hidden states to subquadratic state-space students. Mamba-in-Llama (Wang et al., 2024) interleaves Mamba layers with surviving attention layers in a hybrid student. These works establish that Transformer linearization is feasible, but they do not compare xLSTM [1:0] and Gated DeltaNet under the same teacher, data, scaffold, and optimization recipe. Section 2.2 isolates this matched plug-in comparison.

Table 17: Shared Training Parameters for Time Series Foundation Models across scale

Setting	Value
Positional Encoding	NoPE
Conv Kernel Size	4
Context size	8192
Patch Size	32
Gradient Clipping	1.0
Optimizer	AdamW
LR Scheduler	Cosine + Warmup
Warmup %	3 %
Weight decay	0.1
Learning rate	1.2e-3
Effective Batch Size	256
Num Steps	500,000
Activation Function	SwiGLU

Table 18: Training hyperparameters for synthetic task experiments.

Setting	Value
Hidden Size	128
Num Layers	2
Num Heads	4
Positional Encoding	NoPE
Training Sequence Length	up to 128
Evaluation Sequence Lengths	128, 512, 2048
Optimizer	AdamW
LR Scheduler	Cosine + Warmup
Warmup %	3 %
Weight Decay	{1e-1, 1e-3, 1e-4}
Learning Rate	{1e-3, 3e-4, 1e-4}
Gradient Clipping	1.0
Batch Size	256
Num Steps	50,000
Num Seeds	5